THE ANNALS OF "DUNAREA DE JOS" UNIVERSITY OF GALATI
FASCICLE V, TEHNOLOGIES IN MACHINE BULDING, ISSN 1221-4566
2000

THE GRAPHIC METHOD FOR THE STUDY OF RECIPROC ENVELOPED SURFACES WITH POINT OF CONTACT II –THE HOBBING-CUTTER - COMPARATIVE APPLICATIONS

S.l.ing. Ioan Baicu
Prof.Dr.Ing. Nicolae Oancea
Universitatea "Dunarea de Jos" din Galati

ABSTRACT

In the paper are presented examples of application of the graphic "identification" method for certain concrete cases: the hobbing-cutter for a shaft with a square crossing-section, the hobbing-cutter for a splined-shaft. There are put out the errors face to the analytic methods and it concludes that this identification graphic method can be used with remarcable results

1. Introduction

It was suggested (4), (5), a new method based on an original soft in AutoCAD programming medium for the profiling of the snail-tools, reciproc enveloped with a whire of surfaces (cylindrical or helical), having the disjunct axis face to the helicoid axis representing the primary periphal surface of the snail-tool.

In the following lines, there are also proposed for illustration applications of the graphic algorithm, on the basis of some original soft products realised in AutoLISP language, in accordance with the analytic solutions of the same problem, in order to point out the quality of the new proposed method.

The numerical validity, by one of the known analytic methods, of the new method of profiling the snail-tools generating by winding, may confer the security in its general use, allowing the choise, in accordance with the concrete case of the easier way, at a given moment, of the method of profiling this kind of tool.

2.The hobbing – cutter for a shaft with a square cross-section

The first numeric application refers to profiling the snail-tool for the generation of a shaft with a square profile, figure1.

The resolution of the problem requests in a first step, the numeric profiling of the rack reciproc profiles Σ.

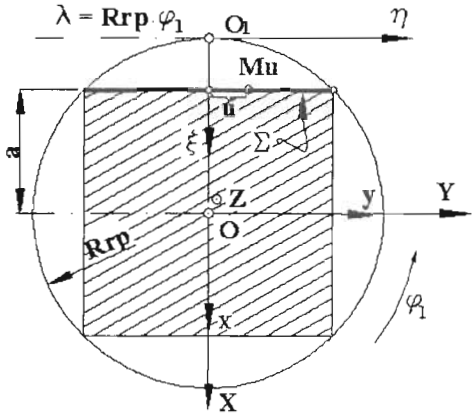

Fig.1. The square shaft

The kinematic of the generation process includes the motions:

$$x = \omega_3^T(\varphi_1)\cdot X, \qquad (1)$$

representing the rotation motion of the system **XYZ**, associated to the profiles whire Σ;

$$x = \xi + a,$$

$$a = \left\| -R_{rp} \quad -R_{rp}\cdot\varphi_1 \quad 0 \right\|, \qquad (2)$$

representing the translation motion of the system ξμζ, solidary to the rack-tool, as absolute motions, comparing to the fixed system of reference, **xyz**, see figure 1, also.

On the basis of the absolute motions (1) and (2), it is established the relative movement

$$\xi = \omega_3^T(\varphi_1)\cdot X - a, \tag{3}$$

from which, knowing the equations of the flank Σ,

$$\Sigma: x = -a;\ y = u;\ z = t, \tag{4}$$

from (3), is established the family of profiles

$$\begin{Vmatrix}\xi\\ \eta\\ \zeta\end{Vmatrix} = \begin{Vmatrix}\cos\varphi_1 & -\sin\varphi_1 & 0\\ \sin\varphi_1 & \cos\varphi_1 & 0\\ 0 & 0 & 1\end{Vmatrix}\cdot\begin{Vmatrix}-a\\ u\\ t\end{Vmatrix} - \begin{Vmatrix}-R_{rp}\\ -R_{rp}\cdot\varphi_1\\ 0\end{Vmatrix}, \tag{5}$$

or, after developments, in form:

$$(\Sigma)_{\varphi_1}\begin{cases}\xi = -a\cdot\cos\varphi_1 - u\cdot\sin\varphi_1 + R_{rp};\\ \eta = -a\cdot\sin\varphi_1 + u\cdot\cos\varphi_1 + R_{rp}\cdot\varphi_1;\\ \zeta = t.\end{cases} \tag{6}$$

The envelope of the family of profiles (6) is established by associating to these equations the condition of winding, which, on the basis of the first theoreme GOHMAN, is established from

$$\vec{N}\times\vec{R}_{\varphi_1} = 0, \tag{7}$$

where:

$\vec{N}_\Sigma$ - is the normal to the surface Σ, (4);

$\vec{R}_{\varphi_1}$ - vector, having the direction of speed in the relative motion of the systems of reference ξη face to **XY**,

$$R_{\varphi_1} = \frac{dX}{d\varphi_1}, \tag{8}$$

and $X = \omega_3(\varphi_1)[\xi + a]$, (9)

the "reverse" motion (see (3)). By differentiation, it gets to the expression

$$R_{\varphi_1} = \dot{\omega}_3(\varphi_1)[\xi + a] + \omega_3(\varphi_1)\cdot\dot{a}_{\varphi_1}, \tag{10}$$

or, after the replacement of the matrix ξ from (3),

$$R_{\varphi_1} = \dot{\omega}_3(\varphi_1)\cdot\omega_3^T(\varphi_1)\cdot X + \omega_3(\varphi_1)\cdot\begin{Vmatrix}0\\ -R_{rp}\\ 0\end{Vmatrix}, \tag{11}$$

After replacements and developments, results the condition of winding:

$$u = R_{rp}\cdot\sin\varphi_1, \tag{12}$$

The assembly of these equations (6) and (7) represents the intermediary surface – the rack reciproc enveloped of the square-shaft-**I**,

$$I\begin{cases}\xi = -a\cdot\cos\varphi_1 + R_{rp}\cdot\cos^2\varphi_1;\\ \eta = -a\cdot\sin\varphi_1 + R_{rp}\cdot\sin\varphi_1\cdot\cos\varphi_1 + R_{rp}\cdot\varphi_1;\\ \zeta = t.\end{cases} \tag{13}$$

with t and φ_1 variable parameters.

What we know being, now, the cylindrical surface of the rack's flank, there can be established the equations of the primary-periphal surface of the snail-tool (see figure2), where are represented the new systems of reference:

$\mathbf{x_0y_0z_0}$ – is the fixed reference system, having the axis $\mathbf{y_0}$ superposed to the axis of the snail-tool;

$\mathbf{X_1Y_1Z_1}$ – mobil system, solidary to the primary-periphal surface of the snail-tool;

$\mathbf{A_{12}}$ – the distance between the axis of the snail-tool and the semi-product's axis.

The other systems of reference were previously defined (see figure1).

The motion's assembly, defining the kinematic of generation with the snail-tool, includes:

- the rotation motion of the primary periphal surface of the snail-tool;

$$x_0 = \omega_2^T(\varphi_2)\cdot X_1; \tag{14}$$

- translation of the system of reference attached to the rack,

$$\xi = x - a_1,\quad a_1 = \begin{Vmatrix}-R_{rs}\\ -\lambda\\ 0\end{Vmatrix}, \tag{15}$$

- the connection between the motion parameters

$$\lambda = p\cdot\varphi_2\cdot\cos\omega, \tag{16}$$

- the connection between the fixed systems of reference, **xyz** and $\mathbf{x_0y_0z_0}$,

$$x_0 = \beta(x - c),\ \text{where}$$

$$\beta = \begin{Vmatrix}1 & 0 & 0\\ 0 & \cos\omega & -\sin\omega\\ 0 & \sin\omega & \cos\omega\end{Vmatrix},\ c = \begin{Vmatrix}-(R_{rp}+R_{rs})\\ 0\\ 0\end{Vmatrix}, \tag{17}$$

- ω - angle of inclination of the snail-tool's axis.

Thus, from (14), (15) and (17), may be established the family of intermediary surfaces in the system of reference of the snail-tool:

$$X_1 = \omega_2(\varphi_2)\cdot\beta\cdot[\xi + a_1 - c]$$

$$(I)_{\varphi_2}\begin{cases}X_1 = [\xi + R_{rs}]\cdot\cos\varphi_2 - [\eta - p\cdot\varphi_2\cdot\cos\omega]\cdot\\ \cdot\sin\varphi_2\cdot\sin\omega - \zeta\cdot\sin\varphi_2\cdot\cos\omega;\\ Y_1 = [\eta - p\cdot\varphi_2\cdot\cos\omega]\cdot\cos\omega - \zeta\cdot\sin\omega;\\ Z_1 = [\xi + R_{rs}]\cdot\sin\varphi_2 + [\eta - p\cdot\varphi_2\cdot\cos\omega]\cdot\\ \cdot\cos\varphi_2\cdot\sin\omega + \zeta\cdot\cos\varphi_2\cdot\cos\omega.\end{cases} \tag{18}$$

The envelope of the family of surfaces $\mathbf{(I)_{\varphi 2}}$ is established by associating to the equations (18), where ξηζ have the significances given by (13), the condition of winding GOHMAN [1], specifies

$$\vec{N}_1\cdot\vec{R}_{\varphi_2} = 0 \tag{19}$$

where:

$\vec{N}_1$ - is the normal to the intermediary surface (13),

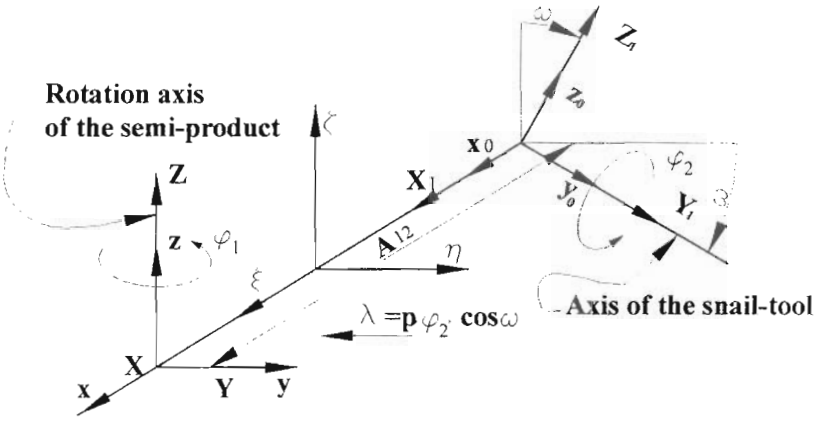

Fig.2. Reference systems

$$\bar{N} = \begin{vmatrix} \bar{i} & \bar{j} & \bar{k} \\ a \cdot \sin\varphi_1 - R_{rp} \cdot \sin(2 \cdot \varphi_1) & -a \cdot \cos\varphi_1 - R_{rp} \cdot \cos(2 \cdot \varphi_1) & 0 \\ 0 & 0 & 1 \end{vmatrix}, \quad (20)$$

$\vec{R}_{\varphi 2}$ – the vector speed in the relative motion of a point from the system of reference $\mathbf{x_1 y_1 z_1}$ face to the system $\xi\eta\varsigma$,

$$R_{\varphi 2} = \frac{d\xi}{d\varphi_2}, \quad (21)$$

and $\xi = \beta^T \cdot \omega_2^T(\varphi_2) \cdot X_1 - a_1 + c.$ (22)

As a result, after differentiation and replacement of the matrix $\mathbf{X_1}$ it arrives to the form

$$R_{\varphi 2} = \beta^T \cdot \dot{\omega}_2^T(\varphi_2) \cdot [\omega_2(\varphi_2) \cdot \beta(\xi + a_1 - c)] - \begin{Vmatrix} 0 \\ -p \cdot \cos\omega \\ 0 \end{Vmatrix}, \quad (23)$$

After developments, the matrix $R_{\varphi 2}$, associated to the vector $\vec{R}_{\varphi 2}$, may be brought to the form

$$R_{\varphi 2} = \begin{Vmatrix} [\eta - p \cdot \varphi_2 \cdot \cos\omega] \cdot \sin\omega + \zeta \cdot \cos\omega \\ -[\xi + R_{rs}] \cdot \sin\omega + p \cdot \cos\omega \\ -[\xi + R_{rs}] \cdot \cos\omega \end{Vmatrix}, \quad (24)$$

where ξ, η and ζ have the significances given by (6).

The assembly of equations (18)-(19)-(20)-(24) represents the primary periphal surface of the snail-tool.

THE AXIAL SECTION OF THE SURFACE S

Technological reasons connected to the measure of the surface S impose the knowledge of its axial sections. From (18), results the axial section $\mathbf{S_A}$, for $\mathbf{Z_1} = 0$, namely (25)

$$[\xi + R_{rs}] \cdot \sin\varphi_2 + [\eta - p \cdot \varphi_2 \cdot \cos\omega] \cdot \cos\varphi_2 \cdot \sin\omega + \zeta \cdot \cos\varphi_2 \cdot \cos\omega = 0. \quad (26)$$

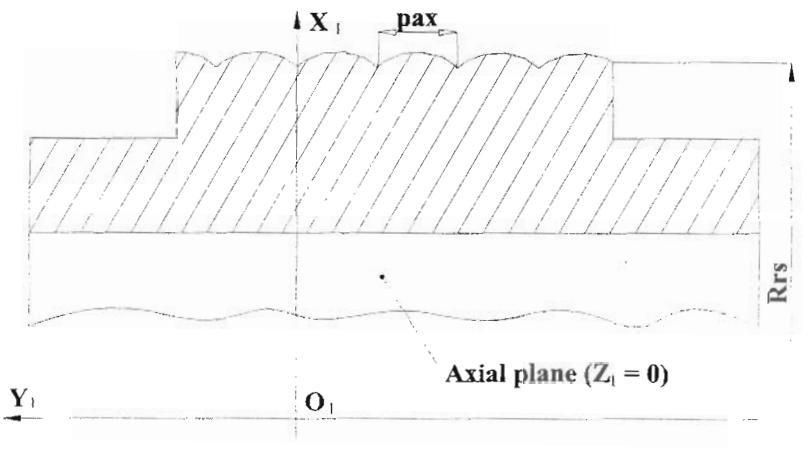

Fig.3. The axial section of the snail-tool

Table 1

The axial section's coordinates	
X_1 [mm]	Y_1 [mm]
50.042425	-11.092479
50.106043	-11.026974
50.190786	-10.938148
50.254247	-10.870085
50.40185	-10.709157
:	:
:	:
50.40185	10.709157
50.254247	10.870085
50.190786	10.938148
50.106043	11.026974
50.042425	11.092479

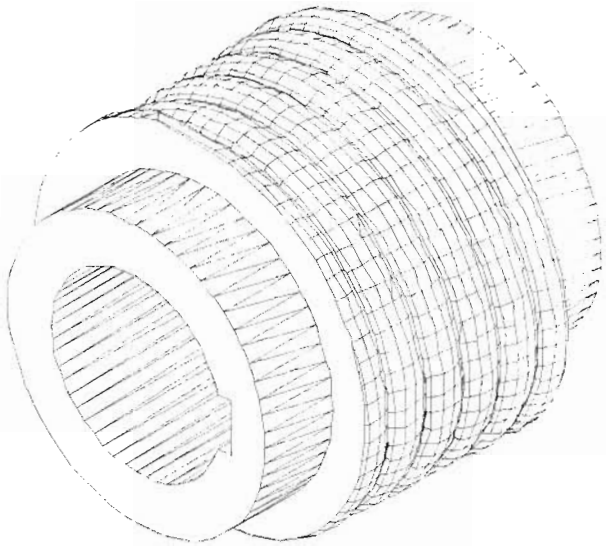

Fig.4. The snai-tool – the solid model of the primary snail

In figure 3 and table 1, are presented, both the form and coordinates of the axial section of the
snail-tool, calculated in accordance with the previous presented algorithm, for

$$a = 10mm;\ R_{rp} = a \cdot \sqrt{2};$$

$$R_{rs} = 50mm;\ p = \frac{R_{rp}}{4};\ tg\omega = \frac{R_{rp}}{4 \cdot R_{rs}}, \qquad (27)$$

on the basis of an original soft, dedicated to these applications.

In order to prove the quality of the used methods, in accordance with the algorithm presented in (6), in figure 4, is represented the solid model of the snail-tool (pointing out its primary-periphal surface).

In figure 5a and the table2, are presented both the form and the axial coordinates of the snail-tool "identified" in accordance with the graphic algorithm, starting from the solid model of the snail-tool.

In figure 5b is presented the axial section's form, analytic established. The profile symmetry
has permitted to represent only half of the profile.

On the purpose of comparing the results, established by the two methods – the analytic method and the graphic method, are compared the measures of the axial section's coordinates (X_1) established to identical values of the coordinates (Y_1), see table 2.

NOTE:

It is obviously, the error of 10^{-4}mm, established in the case of the graphic identification of coordinates, in accordance with the presented algorithm (6), may be considered satisfactory.

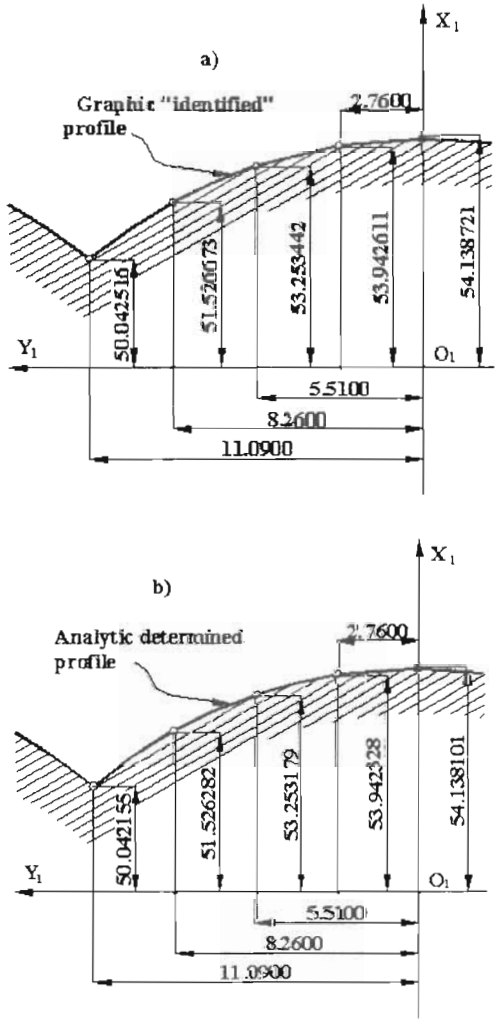

Fig.5. Axial sections, determined graphic a) and analytic b).

Tabelul 2

Coordonatele "identificate"		Coordonatele "analitice"		Eroarea
X_{1i} [mm]	Y_{1i} [mm]	X_1 [mm]	Y_1 [mm]	$\Delta X_1 = X_{1i} - X_1$
50.042516	-11.0900	50.042155	-11.0900	0.000361
50.106171	-11.0400	50.105996	-11.0400	0.000175
50.190842	-10.9900	50.190519	-10.9900	0.000323
50.254361	-10.9400	50.253949	-10.9400	0.000412
50.401931	-10.8900	50.40169	-10.8900	0.000241
:	:	:	:	:
54.138721	0	54.138101	0	0.00062
:	:	:	:	:
50.401931	10.8900	50.40169	10.8900	0.000241
50.254361	10.9400	50.253949	10.9400	0.000412
50.190842	10.9900	50.190519	10.9900	0.000323
50.106171	11.0400	50.105996	11.0400	0.000175
50.042516	11.0900	50.042155	11.0900	0.000361

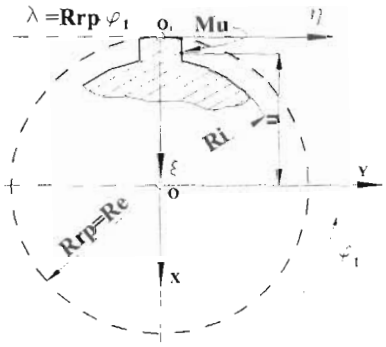

Fig.6. Splined shaft

3.The hobbing – cutter for a splined – shaft

It is presented, a new example related to the figure 6, where is pointed out the cross-section of a splined-shaft with parallel flanks. Knowing the equations of the flank Σ to be generated

$$\Sigma: \; X = -u; \;\; Y = a; \;\; Z = t \;\; , \qquad (28)$$

with **u** and **t** variable parameters, from (3), are inferred the equations of profiles family:

$$(\Sigma)_{\varphi 1} \begin{cases} \xi = -u \cdot \cos\varphi_1 - a \cdot \sin\varphi_1 + R_{rp}; \\ \eta = -u \cdot \sin\varphi_1 + a \cdot \cos\varphi_1 + R_{rp} \cdot \varphi_1. \end{cases} \qquad (29)$$

In concordance with (6), the winding condition is

$$u = R_{rp} \cdot \cos\varphi_1. \qquad (30)$$

and, from here, result the equations of the rack's flank:

$$I \begin{cases} \xi = -R_{rp} \cdot \cos^2\varphi_1 - a \cdot \sin\varphi_1 + R_{rp}; \\ \eta = -R_{rp} \cdot \sin\varphi_1 \cdot \cos\varphi_1 + a \cdot \cos\varphi_1 + R_{rp} \cdot \varphi_1; \\ \zeta = t. \end{cases} \qquad (31)$$

On the basis of the analytic algorithm presented (see paragraph2), it is established, starting from the equations of the intermediary surface **I** (30), the surfaces family $(\mathbf{I})_{\varphi 2}$, in the reference system of the snail-tool:

$$(I)_{\varphi 2} \begin{cases} X_1 = [\xi + R_{rs}] \cdot \cos\varphi_2 - [\eta - p \cdot \varphi_2 \cdot \cos\omega] \cdot \sin\varphi_2 \cdot \\ \cdot \sin\omega - \zeta \cdot \sin\varphi_2 \cdot \cos\omega; \\ Y_1 = [\eta - p \cdot \varphi_2 \cdot \cos\omega] \cdot \cos\omega - \zeta \cdot \sin\omega; \\ Z_1 = [\xi + R_{rs}] \cdot \sin\varphi_2 + [\eta - p \cdot \varphi_2 \cdot \cos\omega] \cdot \cos\varphi_2 \cdot \\ \cdot \sin\omega + \zeta \cdot \cos\varphi_2 \cdot \cos\omega. \end{cases} \qquad (32)$$

Table 3

Coordinates of the axial section	
X_1 [mm]	Y_1 [mm]
54.967618	6.009708
54.923013	5.993791
54.90816	5.985332
54.893304	5.976885
54.878382	5.967986
:	:
:	:
50.209422	4.071427
50.126960	4.060374
50.071215	4.051126
50.008376	4.041497
50.008743	4.036022

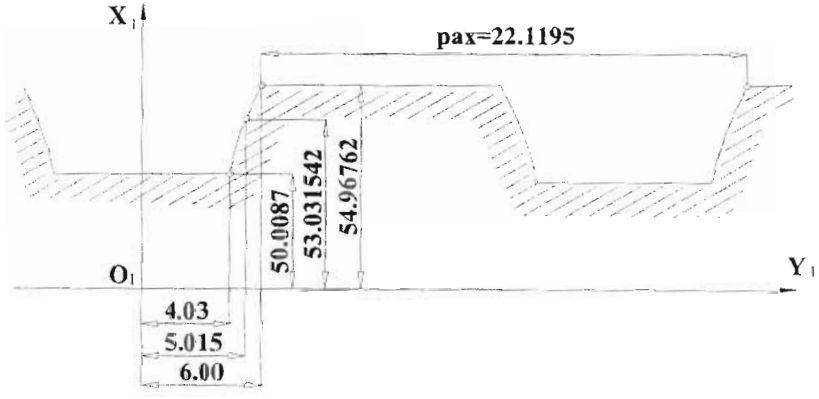

Fig.7. The axial section of the snail-tool

Also, it is established the vector $\bar{R}_{\varphi 2}$,

$$R_{\varphi 2} = \begin{Vmatrix} [\eta - p \cdot \varphi_2 \cdot \cos\omega] \cdot \sin\omega + \zeta \cdot \cos\omega \\ -[\xi + R_{rs}] \cdot \sin\omega + p \cdot \cos\omega \\ -[\xi + R_{rs}] \cdot \cos\omega \end{Vmatrix}, \quad (33)$$

as well as the director parameters of the normal to the surface **I** (31),

$$\begin{cases} N_\xi = -R_{rp} \cdot \cos(2 \cdot \varphi_1) - a \cdot \sin\varphi_1 + R_{rp}; \\ N_\eta = R_{rp} \cdot \sin(2 \cdot \varphi_1) + a \cdot \cos\varphi_1; \\ N_\zeta = 0. \end{cases} \quad (34)$$

On the basis of an original soft, for $R_e = 28mm; R_i = 24mm; a = 4mm; R_{rs} = 50mm$, in figure 7 and table 3, is presented both the form and the coordinates of the axial section of the snail-tool.

In figure 8, is presented the solid model of the snail-tool for the analysed shaft, built in accordance with the algorithm.

In figure 9 and table 4, are presented both the form and the coordinates graphic identified of an axial section of the solid model previously presented, in accordance with those established by the analytic method.

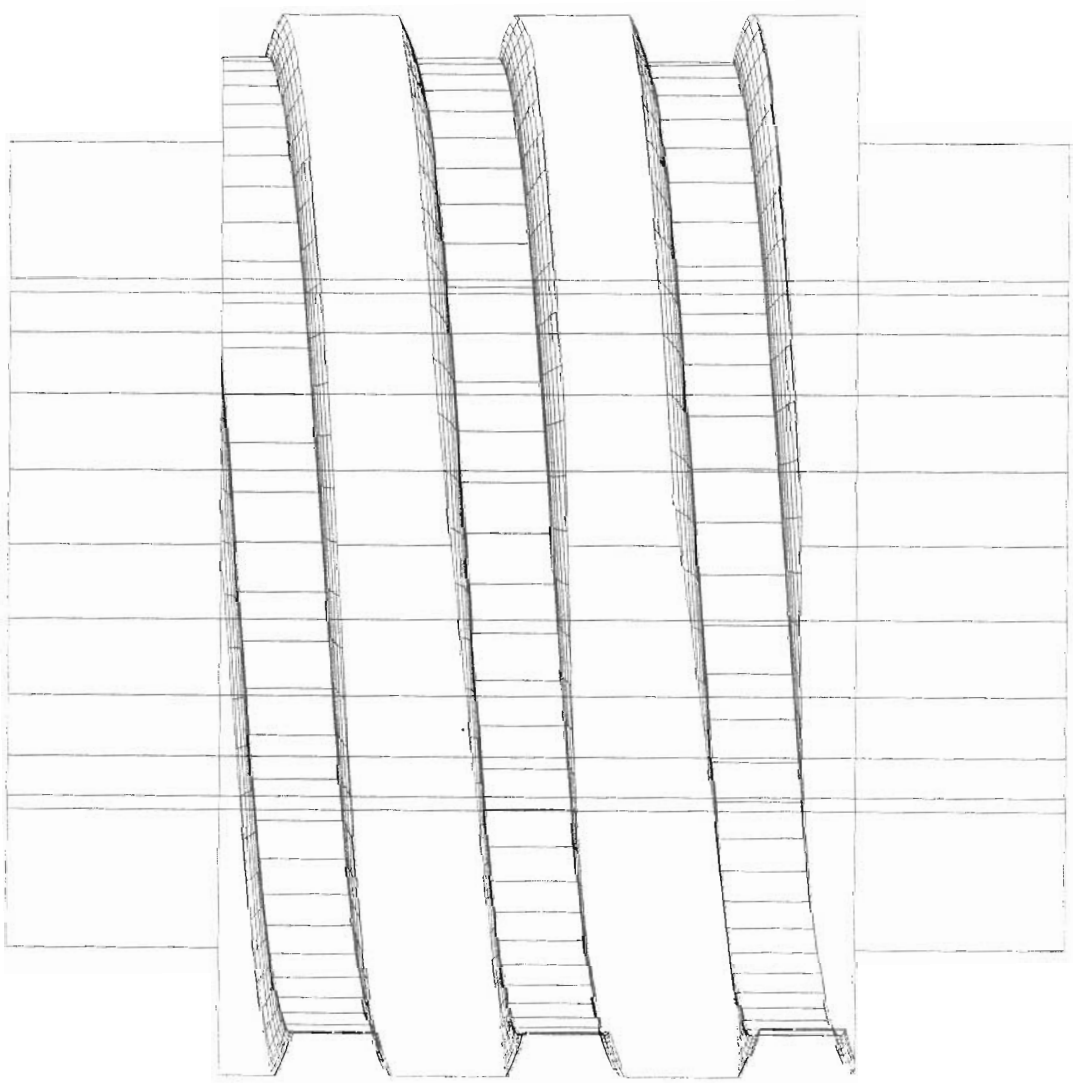

Fig.8. Solid model of the primary worm of the tool

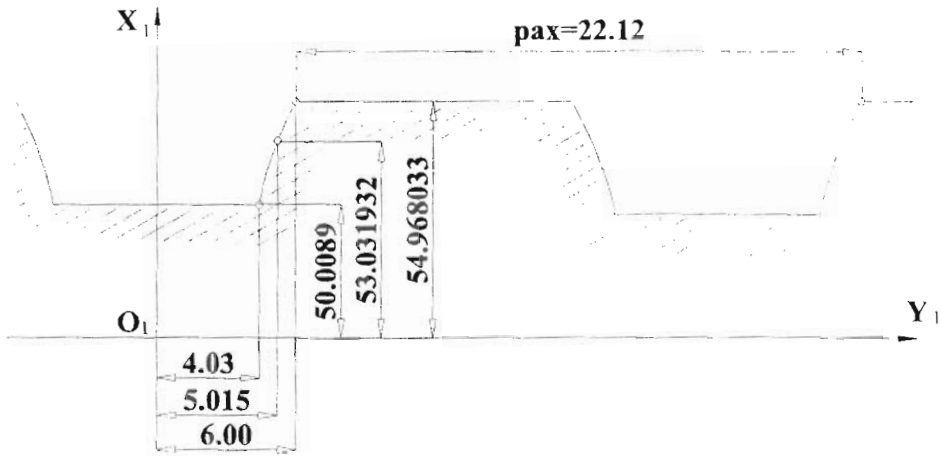

Fig.9. The axial section numerically identified

Table 4

"Identified" coordinates		"Analytic" coordinates		Profile error
X_{1i} [mm]	Y_{1i} [mm]	X_1 [mm]	Y_1 [mm]	$\Delta X_1 = X_{1i} - X_1$
54.968033	6	54.96762	6	0.000415
54.923395	5.99	54.92301	5.99	0.000382
54.908586	5.98	54.90816	5.98	0.000426
54.893413	5.97	54.8933	5.97	0.000109
54.878809	5.96	54.87838	5.96	0.000427
:	:	:	:	:
:	:	:	:	:
50.209678	4.07	50.20942	4.07	0.000256
50.127251	4.06	50.12696	4.06	0.000291
50.071577	4.05	50.07122	4.05	0.000362
50.008789	4.04	50.00838	4.04	0.000413
50.008916	4.03	50.00874	4.03	0.000173

4. Conclusions

The presented algorithm, on the basis of the original soft developped in AutoLISP programming medium, represents an accurate method, rapid and extremely lucrative.

The precision of the method is very large, comparative to that of the analytical method.

Even more, the method is extremely eloquent and, obviously, eliminates from the beginning the possible glaring errors.

5. References

[1] **F.L. litvin** – *"Theory of Gearing"*, Reference Publication, Washingthon DC, 1993

[2] **N. Oancea, V.G. Oancea** – *"Geometrical modeling of Surface Generation through wraping"*, Journal of Manufacturing Science and Engineers, vol.221, part C, p.559-566.

[3] **N. Oancea** – *"Metode numerice pentru profilarea sculelor"*, Universitatea Dunarea de Jos din Galati, vol. I-VII, 1999-2000.

[4] **I. Baicu, N. Oancea** – *"Algoritm pentru identificarea numerica a profilurilor in infasurare generate prin metoda grafica II – scula de tip roata"* , Buletin stiintific, seria C, vol. XV, p.189-194, Universitatea de Nord, Baia Mare, 2001.

[5] **N. Oancea, I. Baicu** – *"Algoritm pentru identificarea numerica a profilurilor in infasurare generate prin metoda grafica I – scula cremaliera"* , Buletin stiintific, seria C, vol. XV, p.305-312, Universitatea de Nord, Baia Mare, 2001.

[6]. **N. Oancea, I. Baicu** – *The grafic method for the study of reciproc enveloped surfaces with point of contact. I – the hobbing cutter – algoritm* –", The Annals of "Dunarea de Jos" University of Galati, Fascicle XIV Mechanical Engineering, ISSN 1224-5615, 2001.

METODA GRAFICĂ PENTRU STUDIUL SUPRAFEŢELOR RECIPROC ÎNFĂŞURĂTOARE CU CONTACT PUNCTIFORM II – FREZA MELC – APLICAŢII COMPARATIVE -

(Rezumat)

În această lucrare sunt prezentate exemple de aplicare a metodei grafice de identificare pentru câteva cazuri concrete: freza melc pentru un arbore cu secţiune transversală pătrată, freza melc pentru un arbore canelat cu caneluri cu flancuri paralele.

Sunt comparate rezultatele obţinute prin metoda grafică şi analitică şi se constată că diferenţele de ordinul a 10^{-4} mm pot duce la concluzia că metoda de „identificare" grafică poate fi utilizată cu rezultate remarcabile.

LA MÉTHODE GRAPHIQUE POUR L'CÉTUDE DE RECIPROC A ENVELOPPÉ DES SURFACES AVEC LE POINT DE CONTACT II - LE FRAISER-COUPEUR - DES APPLICATIONS COMPARATIVES

(Resume)

Dans le papier sont présentés des exemples de l'application de la méthode graphique d'"identification" pour certains cas concrets: le fraisage - coupeur pour un axe avec un croisement-section carrée, le fraiser-coupeur pour éclissé - axe On met dehors le visage d'erreurs aux méthodes analytiques et il conclut que cette méthode graphique d'identification peut être utilisée avec des résultats remarquables.